Long-term Stability of ICPCVD a-Si Under Prolonged Heat Treatment

Kirsten L. Brookshire, Mariusz Martyniuk, K.K.M.B. Dilusha Silva, Yinong Liu, and Lorenzo Faraone
University of Western Australia

Abstract- Inductively coupled plasma enhanced chemical vapor deposited (ICPCVD) a-Si is used as a structural material in many microelectromechanical systems (MEMS). For a-Si to function as a sound structural component, the material must display long term mechanical stability. This paper evaluates the Young's modulus, hardness, and residual stress of a-Si under prolonged heat treatment. It is found that Young's modulus and hardness are not impacted by heat treatment, while the residual stress becomes more tensile with increased annealing time. Increased tensile stress is a result of hydrogen offgassing which can lead to improved film stability [1].

Index Terms—ICPCVD, Young's modulus, hardness, residual stress, bi-layer, thin film, a-Si

I. Introduction

A popular material for microelectromechanical systems (MEMS) is a-Si, both for structural and optical applications. The majority of studies for Si-based thin films focus on SiN_x or SiC [2, 3]. Extensive studies of SiN_x long-term stability have been conducted by others [2-5], as well as for crystalline Si. However, the body of work done on a-Si (a-Si:H or pc-Si:H) is sparse.

The research for a-Si thin films focuses primarily on the deposition conditions and how they relate to hydrogen concentration in the resultant film [6-8], or the optical and electron transport properties of the film [9-18]. Some papers have also reported on thermomechanical properties [19] and residual stress [1, 20]. However, the long-term stability of a-Si thin films as a structural component for MEMS is largely unreported.

The deposition conditions for this study have been preselected as giving a film with desirable optical properties for subsequent use as a structural and optical layer in microspectrometer concept developed at the University of Western Australisa [21]. The study focuses on the long-term stability of these films as evaluated through the elastic modulus, hardness, and residual stress.

K. L. B. Author is with the Microelectronics Research Group (MRG) at the University of Western Australia, Crawley, WA 6008 Australia (phone: +61 409 027 988; e-mail: kirsten.brookshire@research.uwa.edu.au).

M.M. Author is with MRG at the University of Western Australia, Crawley, WA 6008 Australia (e-mail: mariusz.martyniuk@uwa.edu.au).

K. K. M. B. D. S. Author is with MRG at the University of Western Australia, Crawley, WA 6008 Australia (e-mail: dilusha.silva@uwa.edu.au).

Y.L. Author is with the school of Mechanical and Chemical Engineering at the University of Western Australia, Crawley, WA 6008 Australia (e-mail: yinong.liu@uwa.edu.au).

L. F. Author is with the MRG at the University of Western Australia , Crawley, WA 6008 Australia (e-mail: lorenzo.faraone@uwa.edu.au).

II. Experimental

Samples were deposited in a SenTech SI 500 D ICPCVD tool. Three samples of a-Si on 300 um Si (100) substrate were used for nanoindentation studies. Twenty samples of a-Si on 70 um Si (100) substrate were used for the thin film induced substrate bending analysis. The deposition conditions are given in Table I. The resultant films were 1 um in thickness. Samples were annealed using a conventional annealing oven in an Ar atmosphere for times ranging from 5 minutes to 48 hours.

A. Nano-indentation

Nano-indentation, performed using a Hysitron 950 TriboIndenter with a Berkovich tip, was used to evaluate the Young's modulus and hardness of the deposited a-Si films. A series of 49 indentations (a 7 by 7 array of points with 20 um spacing) was used to indent a standard fused quartz sample throughout the data collection. A standard indentation load profile was used. The maximum load ranged from 500 uN to 11,500 uN. Indentation into the standard was used to calculate the tip area function, with regular calibration of the tip area function performed to aid qualitative data analysis.

Nano-indentation was also performed (in the same manner as described above) on the test samples. These samples consisted of: a bare, 300 um thick, Si (100) wafer; a-Si samples with annealing times of 60 minutes, 1440 minutes; and a control a-Si sample that underwent no annealing.

The reduced modulus and hardness is calculated by the Hysitron analysis software using the middle 20% to 95% of the unload curve. The unload data is analyzed following the Oliver-Pharr method [22].

The hardness, H, is calculated using

$$H = \frac{P_{max}}{A(h_c)}, \quad (1)$$

where $A(h_c)$ is the calibrated contact area and P_{max} is the maximum indentation load.

The reduced modulus, E_r, is calculated using

$$\frac{1}{E_r} = \left(\frac{1-\upsilon^2}{E}\right)_{sample} + \left(\frac{1-\upsilon^2}{E}\right)_{indenter}, \quad (2)$$

which can be used to extract the Young's modulus of the sample using known values for the sample's Poisson ratio and indenter parameters. For a diamond indenter Young's modulus is 1140 GPa and the Poisson ratio is 0.07 [23]. Poisson ratio for Si is typically 0.27 [24].

TABLE I
DEPOSITION CONDITIONS FOR ICPCVD a-Si

Gas flow		Temperature	Pressure	Power
SiH_4:	He:			
5 sccm	95 sccm	300 °C	4 Pa	26 W

B. Thin film induced substrate bending

Thin film stress was deduced via measurements of thin film induced substrate curvature. Substrate curvature was measured using a Zygo optical profilometer on the 70 um Si (100) wafers prior to deposition. After the films were deposited curvature was again recorded. Finally, samples were annealed for times ranging from 5 minutes to 48 hours and curvature data recorded for a third time.

The residual film stress was evaluated from the substrate curvature using the Stoney equation [25],

$$\sigma_f = \frac{E_s t_s^2}{6(1-\nu_s)t_f}\frac{1}{R_0}, \quad (3)$$

where E_s is the Young's modulus of the substrate, ν_s is the Poisson ratio of the substrate, R_0 is the change in radius of curvature, and t_s and t_f are the substrate and film thickness, respectively.

III. RESULTS & DISCUSSION

IV. Residual Stress

Radius of curvature data collected after ICPCVD of the Si films prior to any annealing, were used to evaluate the distribution of as-deposited residual stress. Fig. 1 shows a histogram of the 20 deposited films, as well as the calculated normal distribution. The normal distribution had a mean residual stress value of -27 MPa and standard deviation of 9 MPa. For the data reported +'ve is indicative of a tensile stressed film and –'ve is indicative of a compressive stressed film. The as-deposited films were slightly compressive.

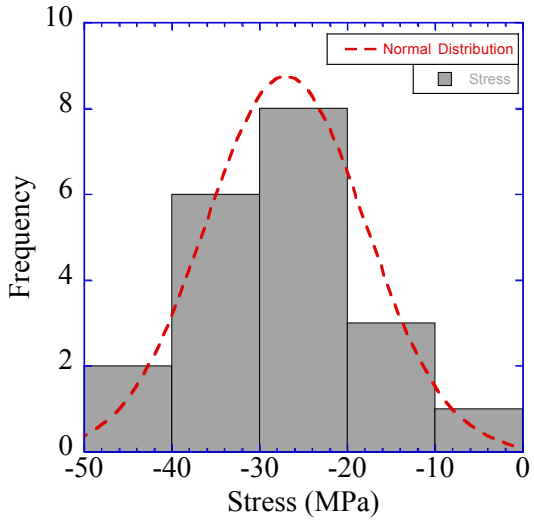

Fig. 1. Histogram of the post deposition stress in 1 um-thick ICPCVD a-Si films. The red line indicates the Normal distribution, with a mean of -27.02 MPa and a standard deviation of 9.11 MPa.

Radius of curvature data were collected after the samples were annealed in Ar at 300 °C for times ranging from 5 minutes to 48 hours. Fig. 2 plots the stress (as calculated via equation 3 from the thin film induced substrate curvature measurements) versus annealing time for a-Si on 70 um Si (100) substrate. The figure shows the films becoming more tensile with anneal time. The data appears to be saturating with annealing time at a maximum tensile film stress value of approximately 400 MPa. However, the films annealed for 48 hours cracked and delaminated. This indicates that between 24 and 48 hours the stress in the films continued to increase, but further study is required to confirm this.

A. Elastic modulus and Hardness

Indentation data collected on the standard fused quartz sample (Fig. 3) shows stable measurement. The limitations of the indenter can also be seen in this data. The hardness shows a trailing off at a contact depth of approximately 50 nm. This trailing is attributable to the indentation size effect. Therefore, in this study we will limit the reporting to indentations deeper than 50 nm.

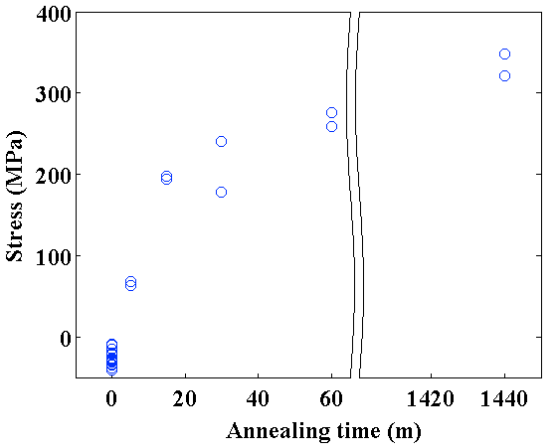

Fig. 2. Plot of stress versus annealing time. Stress is calculated using thin film induced substrate bending. The trend appears to be saturating at a maximum residual stress value of 400 MPa.

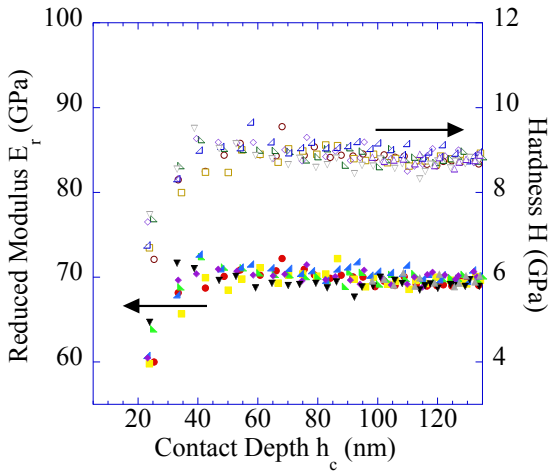

Fig. 3. Indentation of fused quartz sample used to calibrate the tip area function. Indentations taken before, during and after indentation of ICPCVD Si sample do not drift indicating reliable data for the Si samples

The indentation data for the ICPCVD a-Si on 300 um Si (100) wafers are reported in Fig. 4 and Fig. 5. The Young's modulus (calculated from the reduced modulus via Equation 5) as a function of contact depth is shown in Fig. 4. The average Young's modulus of the Si substrate is 175 GPa ± 3 GPa, The average Young's modulus for as-deposited a-Si (excluding the tail region of the data from 0 nm to 50 nm contact depth) ranges from 124 GPa ± 5 GPa to 133 GPa ± 4 GPa. All results are reported in Figure 6. A slight increase in Young's modulus with anneal is observed, but the variation is within the error of the measurement.

Fig. 5 plots the Hardness versus contact depth for the ICPCVD Si films. The hardness for the 300 um Si substrate is 11.4 GPa ± 0.2 GPa. The average hardness for the as deposited a-Si, calculated from results with contact depths greater than 50 nm, ranged from 9.5 GPa ± 0.5 GPa to 10.3 GPa ± 0.4 GPa. All results are reported in Figure 6. The data shows a slight trend towards reduced hardness with annealing time. However, this trend is within the experimental error.

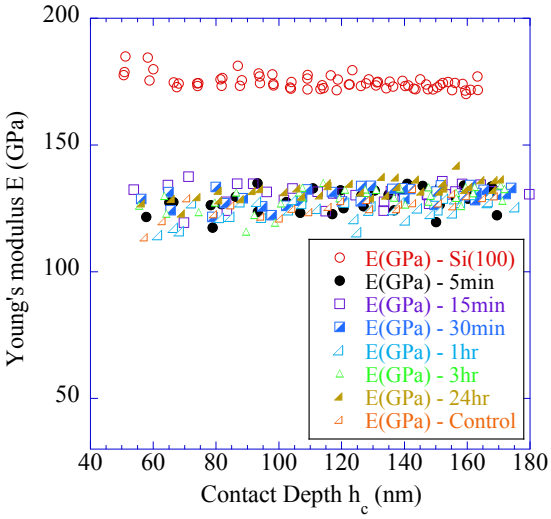

Fig. 4. Plot of Young's modulus versus contact depth for bare 300 um Si (100) substrate and ICPCVD a-Si. The Young's modulus, calculated from the reduced modulus via Equation 5, is 175 GPa for Si (100) substrate and approximately 130 GPa for the deposited a-Si

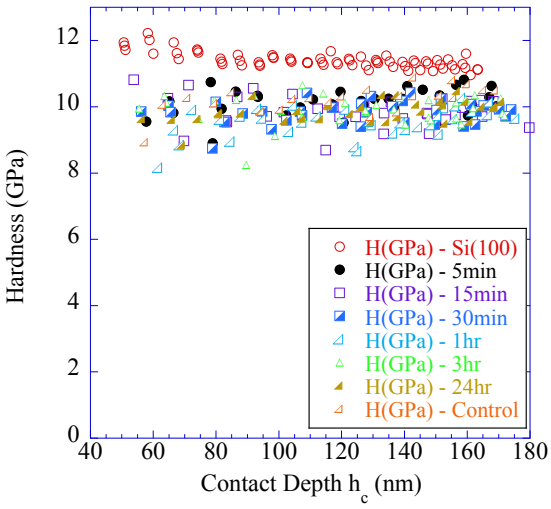

Fig. 5. Plot of hardness versus contact depth for both the bare 300 um Si (100) wafer and ICPCVD a-Si. The hardness of Si (100) wafer is 11.4 GPa while that of the deposited a-Si is approximately 10 GPa.

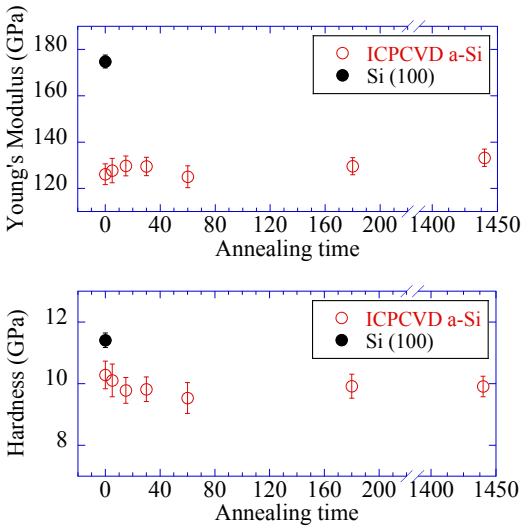

Fig. 6. Plot of Young's modulus (top) and hardness (bottom) versus annealing time for bare 300 um Si (100) substrate and ICPCVD a-Si. The Young's modulus, calculated from the reduced modulus via Equation 5, is 175 GPa for Si (100) substrate and ranges between 133 GPa and 124 GPa for the deposited a-Si.

V. CONCLUSION

The results of this annealing study show that the primary instability associated with long-term exposure to heat of ICPCVD a-Si, is in the residual film stress. The nanoindentation showed that the Young's modulus and hardness of ICPCVD a-Si are not significantly changed by exposure to elevated temperatures in an Ar atmosphere.

The residual film stress changed significantly after only 5 minutes at elevated temperatures. The residual stress in the films appeared to be saturating at a maximum tensile stress value of approximately 400 MPa.

It is believed that this effect of changing residual stress is attributed to Hydrogen outgassing from the sample [1]. Because the samples were in an Ar atmosphere, oxygen entering the films is not a likely reason for the change in film stress. Further evaluation of ICPCVD a-Si in air and oxygen atmospheres is required to confirm this.

ACKNOWLEDGMENTS

This work was partially funded by the Australian Research council (ARC) and the WA State Government. This work was performed in part at the Western Australian node of the Australian National Fabrication Facility and the Australian Microscopy & Microanalysis Research Facility at the Centre for Microscopy, Characterisation & Analysis, The University of Western Australia.

REFERENCES

[1] Y. Q. Fu, J. K. Luo, S. B. Milne, A. J. Flewitt, and W. I. Milne, "Residual stress in amorphous and nanocrystalline Si films prepared by PECVD with hydrogen dilution," *Materials Science and Engineering B-Solid State Materials for Advanced Technology,* vol. 124, pp. 132-137, Dec 2005.

[2] T. F. Retajczyk and A. K. Sinha, "Elastic stiffness and thermal expansion coefficients of various refractory silicides and silicon-nitride films," *Thin Solid Films,* vol. 70, pp. 241-247, 1980.

[3] M. Martyniuk, J. Antoszewski, C. A. Musca, J. M. Dell, and L. Faraone, "Stress in low-temperature plasma enhanced chemical vapour deposited silicon nitride thin films," *Smart Materials & Structures,* vol. 15, pp. S29-S38, 2006.

[4] M. Martyniuk, J. Antoszewski, C. A. Musca, J. M. Dell, and L. Faraone, "Environmental stability and cryogenic thermal cycling of low-temperature plasma-deposited silicon nitride thin films," *Journal of Applied Physics,* vol. 99, Mar 1 2006.

[5] H. Huang, K. Winchester, Y. Liu, X. Z. Hu, C. A. Musca, J. M. Dell*, et al.*, "Determination of mechanical properties of PECVD silicon nitride thin films for tunable MEMS Fabry-Perot optical filters," *Journal of Micromechanics and Microengineering,* vol. 15, pp. 608-614, 2005.

[6] Y. G. Fu, J. K. Luo, S. B. Milne, A. J. Flewitt, and W. I. Milne, "Residual stress in amorphous and nanocrystalline Si films prepared by PECVD with hydrogen dilution," *Materials Science and Engineering B-Solid State Materials for Advanced Technology,* vol. 124, pp. 132-137, Dec 2005.

[7] D. V. Tsu, B. S. Chao, S. R. Ovshinsky, S. Guha, and J. Yang, "Effect of hydrogen dilution on the structure of amorphous silicon alloys," *Applied Physics Letters,* vol. 71, pp. 1317-1319, Sep 8 1997.

[8] C. J. Fang, K. J. Gruntz, L. Ley, M. Cardona, F. J. Demond, G. Muller*, et al.*, "Hydrogen content of a-GE-H and a-SI-H as determined by ir spectroscopy, gas evolution and nuclear-reaction techniques," *Journal of Non-Crystalline Solids,* vol. 35-6, pp. 255-260, 1980 1980.

[9] A. V. Shah, H. Schade, M. Vanecek, J. Meier, E. Vallat-Sauvain, N. Wyrsch*, et al.*, "Thin-film silicon solar cell technology," *Progress in Photovoltaics,* vol. 12, pp. 113-142, Mar-May 2004.

[10] C. H. Park, B. H. Cheong, K. H. Lee, and K. J. Chang, "Structural and electronic-properties of cubic, 2h, 4h, and 6h SIC," *Physical Review B,* vol. 49, pp. 4485-4493, Feb 15 1994.

[11] Y. L. He, C. Z. Yin, G. X. Cheng, L. C. Wang, X. N. Liu, and G. Y. Hu, "The structure and properties of nanosize crystalline silicon films," *Journal of Applied Physics,* vol. 75, pp. 797-803, Jan 15 1994.

[12] G. D. Cody, "The optical absorption edge of a-Si-H," *Semiconductors and Semimetals,* vol. 21, pp. 11-82, 1984 1984.

[13] H. Dersch, L. Schweitzer, and J. Stuke, "Recombination processes in a-Si-H - Spin-dependent photoconductivity," *Physical Review B,* vol. 28, pp. 4678-4684, 1983 1983.

[14] R. A. Street, D. K. Biegelsen, and J. C. Knights, "Defect states in doped and compensated a-SI-H," *Physical Review B,* vol. 24, pp. 969-984, 1981 1981.

[15] J. C. Knights, "Growth-morphology and defects in plasma-deposited a-SI-H films," *Journal of Non-Crystalline Solids,* vol. 35-6, pp. 159-170, 1980 1980.

[16] H. Fritzsche, "Characterization of glow-discharge deposited a-SI-H," *Solar Energy Materials,* vol. 3, pp. 447-501, 1980 1980.

[17] J. C. Knights and R. A. Lujan, "Microstructure of plasma-deposited a-SI-H films," *Applied Physics Letters,* vol. 35, pp. 244-246, 1979 1979.

[18] J. C. Knights, G. Lucovsky, and R. J. Nemanich, "Defects in plasma-deposited a-SI-H," *Journal of Non-Crystalline Solids,* vol. 32, pp. 393-403, 1979 1979.

[19] F. Jansen, M. A. Machonkin, N. Palmieri, and D. Kuhman, "Thermomechanical properties of amorphous silicon and nonstioichiometric silicon-oside films," *Journal of Applied Physics,* vol. 62, pp. 4732-4736, Dec 15 1987.

[20] S. Chang and S. Sivoththaman, "Development of a low temperatureMEMS process with a PECVD amorphous silicon structural layer," *Journal of Micromechanics and Microengineering,* vol. 16, pp. 1307-1313, Jul 2006.

[21] J. Antoszewski, K. J. Winchester, T. Nguyen, A. J. Keating, K. Silva, C. A. Musca*, et al.*, "Materials and processes for MEMS-based infrared microspectrometer integrated on HgCdTe detector," *Ieee Journal of Selected Topics in Quantum Electronics,* vol. 14, pp. 1031-1041, Jul-Aug 2008.

[22] W. C. Oliver and G. M. Pharr, "Measurement of hardness and elastic modulus by instrumented indentation: Advances in understanding and refinements to methodology," *Journal of Materials Research,* vol. 19, pp. 3-20, Jan 2004.

[23] L. Riester, M. K. Ferber, and K. Breder, "Elastic modulus calculations from load/displacement curves using spherical and pointed indenters," in *Nondestructive Evaluation of Ceramics*. vol. 89, C. H. Schilling and J. N. Gray, Eds., ed Westerville: Amer Ceramic Soc, 1998, pp. 337-344.

[24] L. Gan, B. BenNissan, and A. BenDavid, "Modelling and finite element analysis of ultra-microhardness indentation of thin films," *Thin Solid Films,* vol. 290, pp. 362-366, Dec 1996.

[25] G. G. Stoney, "The tension of metallic films deposited by electrolysis," *Proceedings of the Royal Society of London Series a-Containing Papers of a Mathematical and Physical Character,* vol. 82, pp. 172-175, May 1909.